Investigation of Wireless Sensor Deployed on a Rotating Shaft and Its Potential for Machinery Condition Monitoring

Lutfi Arebi, Yibo Fan, Fengshou Gu and Andrew Ball
University of Huddersfield, Queensgate, Huddersfield, HD1 3DH, UK

ABSTRACT

Rotating shafts are the most critical component of rotating machines such as motors, pumps, engines and turbines. Due to their heavy duties, defects are more like developed during operation. There are many techniques used to monitor shaft defects by analysing the vibration of the shaft as well as the instantaneous angular speed (IAS) of the shaft. The signal are measured either using non-contact techniques such as laser-based measurement or indirect measurement such as the vibration on bearing housings. The advancement in low cost and low power Micro Electro Mechanical Systems (MEMS) make it possible to develop an integrated wireless sensor which can be mounted on the shaft. This can make the fault diagnosis of rotating shafts more effective because the sensor can be mounted on the shaft directly. This paper presented a novel integrated wireless accelerometer for rotational parameter measurement. Its performance is benchmarked with that from a shaft encoder. Experimental results show that the wireless acceleration signal has less noise and hence it is more possible for small fault detection.

Keywords: Wireless sensor, Rotating shaft, Instantaneous angular speed, Condition monitoring

1. INTRODUCTION

Rotating shafts are necessary components for many mechanical applications like pumps, engines and turbines. The dynamic behavior of rotating shaft has been studied using static measurement of the vibration. However, it is difficult to evaluate the dynamic behavior of rotating shaft by deploying wired sensors on the shaft. The advent in wireless communication has led to a wide use of wireless concept in various aspects of our life and the development of wireless sensors makes it possible to conduct measurement directly on a rotating shaft.

The challenges of using wireless sensing on rotating shaft have not been adequately addressed. F. Andrés et la [1] used the wireless sensor to identify the crack on a rotating shaft. The majority of papers dealt with theoretical considerations and simulations of this idea. The potential of wireless accelerometer directly deployed on the shaft is not fully investigated.

This study employed wireless modules operating in the UHF spectrum to develop wireless accelerometers from MEMS commercial accelerometer of ADXL. The frequency band used can provide transmission signals with low power consumption and low noise. With the help of radio communication, the wireless sensors can be flexibly deployed at places unsuitable for wired sensors and transmit their collected data to external data repositories. The result of the novel wireless accelerometer node, which was directly mounted on rotating shaft, was presented in this paper. The extracted IAS from wireless sensor was compared with the signal from encoder that is used as benchmark in the validation tests.

2. WIRELESS SENSOR DEVELOPMENT

The wireless accelerometer node used in this research was developed using a MEMS accelerometer ADXL202AE with duty cycle output which can be conditioned conveniently to work wirelessly by the transmitter and receiver modules. The accelerometer is able to measure positive and negative absolute accelerations of ± 2g.

The duty cycle period is adjustable from 0.5 ms to 10 ms via a single resistor (R_{SET}) [2]. The duty cycle outputs are available from X_{OUT} and Y_{OUT} pins. Moreover, the analogue output can be reconstructed by filtering the duty cycle outputs.

The bandwidth of the ADXL202 can be set from 10 Hz to 5 kHz via capacitors C_X and C_Y as shown in Figure 1 [2].

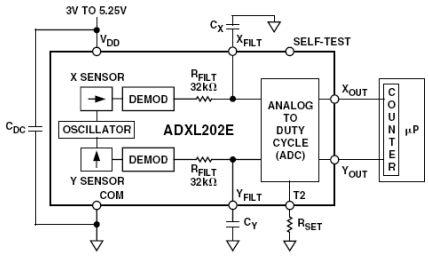

Figure 1 Accelerometer block diagram

2.1 Duty Cycle Signal (DCS)

Duty cycle signal depicted in Figure 2 has a period of T and duty cycle D. The value of D finds out the percent of duty cycle of ON time corresponds to the period time T, 100% being fully ON. A low duty cycle associated to low power due to the power is OFF for most of its time.

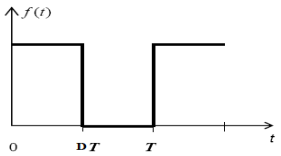

Figure 2 Duty cycle signal with period T and duty cycle D

The DCS resolution is defined as the maximum number of pulses can be fit into DCS period that means 100% [3]. The DCS period is defined as an arbitrarily time period in which DCS take place. It is chosen to suit specific application [3].

The easiest and cheapest way to reconstruct the analogue signal from the duty cycle is to use low-pass filter with cut-off at any frequency below the carrier frequency. Ideally, this filter can remove the high frequency harmonics and only leave the D.C. component. In addition, the filter will allow the duty cycle to be varied at frequencies up to the cut-off frequency and reflect this variation with a corresponding voltage level change in the D.C. output. However, a real filter always allows some portion of the harmonics to pass, which produces ripple in the desired output. A trade-off between harmonic ripple and duty cycle carrier frequency is required during the design of analogue low-pass filter for specific application.

2.2 Circuit Design

The first step in the design is to select the period of duty cycle (T) so that the analogue output can be reconstructed. According the specifications of the accelerometer, T should be in the range from 0.5ms to 0.9ms.

The duty cycle period was adjusted to 0.544ms by the resistor (R_{SET} = 68 KΩ). Therefore frequency of DCS was 1.838 kHz. The bandwidth of the accelerometer was set to 500 Hz by selecting capacitors C_x and C_y to 0.01 μF.

2.2.1 Wireless Accelerometer Operating Description

The DCS signal of the Wireless accelerometer is sent by the transmitter module in radio frequency waves at 418 MHz, as shown in Figure 3a. This radio frequency signal is acquired by the receiver

module shown in Figure 4b and sent to the Sallen-Key low pass filter with cut-off frequency of 131.5 Hz to reconstruct the analogue signal. The analogue signal from the low pass filter is outputted to the data acquisition system (DAS). The signal is sampled at 96000 Hz by DAS and the recorded data is processed using Matlab.

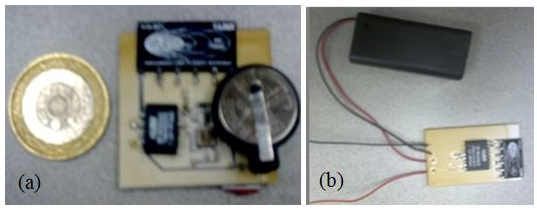

Figure 3 Developed: (a) Wireless Accelerometer node circuit (b) Receiver circuit

2.2.2 Sensitivity of the Wireless Sensor

The +1 g accelerometer output (A) was measured by pointing the x-axis of wireless accelerometer directly to the earth. The sensor then is turned 180° to measure the output at -1 g (B). Using the two duty cycle readings from the oscilloscope, the sensor sensitivity was calculated [2]:

$$Sensitivity\ (S_a) = \frac{A-B}{2g} \quad (1)$$

$$Sensitivity(S_a) = \frac{72.8\%-54.5\%}{2g} = 9.15\%/g$$

Since the voltage supply V_{DD} =3Volts

$$S_a = 9.15\%/g \times 3V = 274.5mV/g = 27.98165\ mV/ms^{-2}$$

2.3 Frequency Response

The frequency response of the wireless accelerometer was evaluated by comparing with a commercial accelerometer with known frequency response.

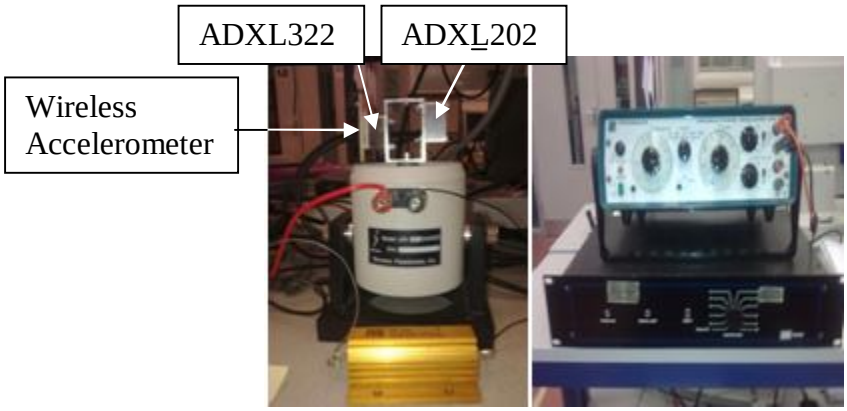

Figure 4 Sensor Calibration using JZK-2 vibrator

Figure 4 gives the calibration system which consists of a JZK-2 model shaker (vibrator), a function generator and amplifier. Two wired accelerometer were used to calibrate the developed wireless accelerometer: One was ADXL202AE, the same type as the wireless sensor; the other was ADXL322. The three accelerometers, as shown in Figure 4, were held by an aluminium rectangular frame and mounted to vibrator.

The vibrator was driven by the amplified sine wave from the signal generator and amplifier unit. The frequency responses of accelerometers to every change in the sine waveform frequency were recorded. Throughout this test, the accelerometer's practical resonant frequency was determined and the signal output with respect to different vibration frequencies was examined.

The outputs of accelerometers were recorded using data acquisition with a sampling frequency of 96 kHz and the results were processed using Matlab. Figure 5(a) shows the amplitude frequency response of the three accelerometers. It can be observed that the response of wireless accelerometer is very close to ADXL322 and noticeable different from ADXL202. This is because the wireless accelerometer was mounted next to ADXL322 accelerometer while the ADXL202 was mounted on the other side of the holder, as shown in Figure 4. Although the bandwidth of both wired accelerometer is 500 Hz, the wireless accelerometer bandwidth is limited by the low pass filter, which is 131.5 Hz.

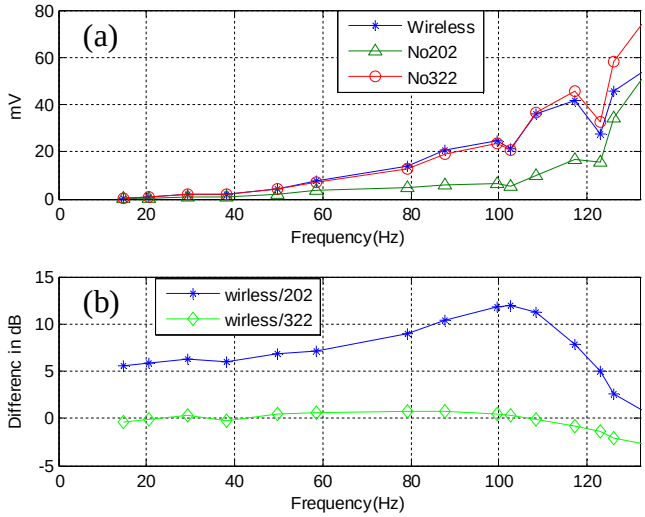

Figure 5 Frequency response comparison between a wireless accelerometer and two wired ones (ADXL202 and ADXL203)

3. EXPERIMENTAL VALIDATION OF THE WIRELESS SENSOR

3.1 Validation Approach

When the wireless accelerometer was mounted directly on a rotating shaft, the dynamic behaviour of a shaft caused the change in machine condition can be monitored. The principle is similar to the measurement of instantaneous angular speed (IAS). Therefore an encoder was employed in this experimental study to benchmark dynamic behavior of the rotating shaft. The validation was conducted by comparing the IAS signals extracted from the wireless accelerometer and encoder.

3.2 Test Rig

The bearing test rig, shown in Figure 6, was employed in this experimental study. It consists of a 3-phase electrical induction motor and a dynamic brake. The motor is connected to the brake by means of four shafts, which are connected by three pairs of flexible couplings and supported by bearings in two bearing housings. The wireless accelerometer was mounted directly on the second shaft while the encoder (type RI32) was mounted with induction motor rotor as shown in Figure 6. The test rig can run at a speed from 60 rpm to 1500 rpm.

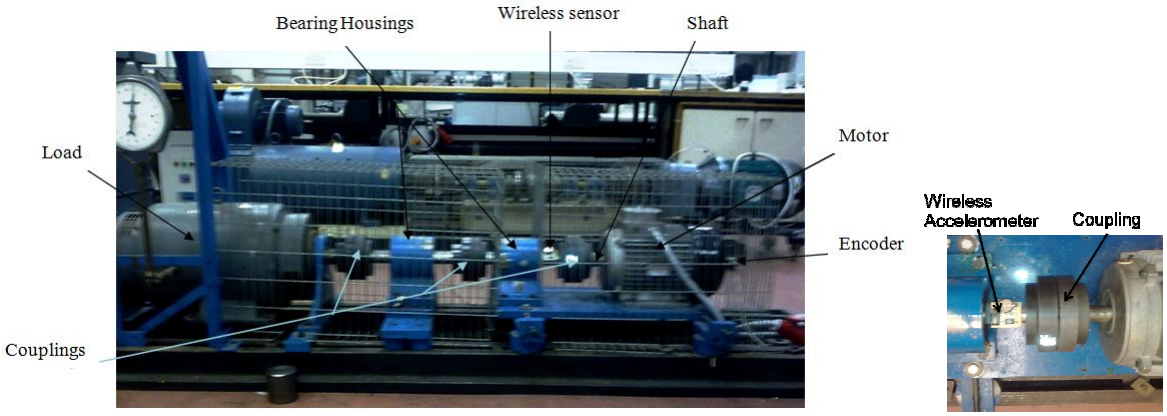

Figure 6 Test Rig and the Installation of Wireless Sensor

3.3 Data acquisition system

While the wireless accelerometer was mounted on the shaft, the receiver, which receives duty cycle signal of the sensor, was connected to Sallen-Key second order active low pass filter with a cut-off frequency of 131.5 Hz. This filter is designed to filter the duty cycle signal in order to reconstruct the analogue form of the signal. Then, the filtered signal was outputted to the data acquisition hardware shown in Figure 7. The sampling frequency was set to 96 kHz. The encoder sensor signal was conditioned and also connected to the data acquisition system. The recorded signals were processed using the software developed in Matlab.

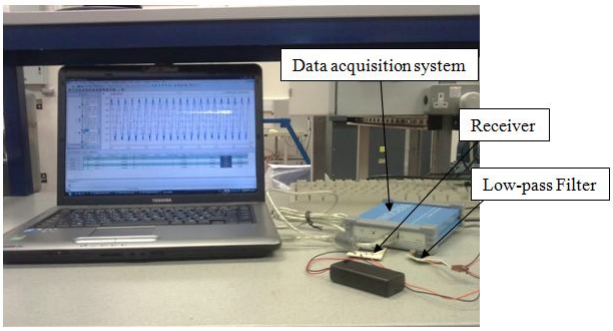

Figure 7 Data Acquisition System

4. EXPERIMENTAL RESULTS AND DISCUSSIONS

Figure 8(a) gives the duty cycle signal of the wireless accelerometer and the extracted analogue signal. The duty cycle signal was filtered using Sallen-key low pass filter and then converted to acceleration signal in the time domain by using developed Matlab code. Figure 8(b) shows a noisy sample to demonstrate the performance of the filter used for converting DCS to analogue signal.

The active low pass filter used to reconstruct the analogue signal from the duty cycle signal limited the band width of accelerometer to 131.5 Hz. Finite impulse response digital filter was applied to the signal in Figure 8(b) to reduce high frequency noise. Figure 9(a) gives the filtered signal when test was conducted at 300 rpm and its spectrum was presented in Figure 9(b) by conducting Fast Fourier Transform (FFT). It can be seen that the frequency of the signal is 5 Hz, the same as the shaft rotating frequency.

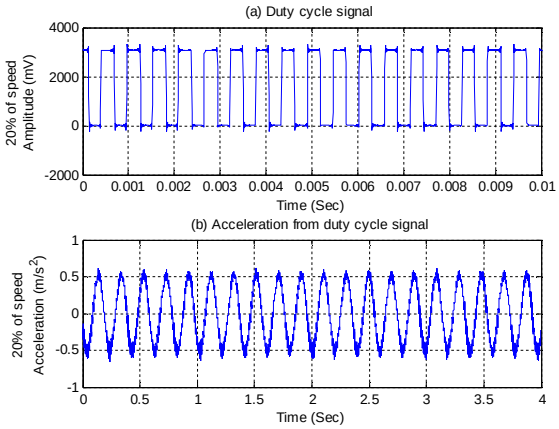

Figure 8 Output of wireless accelerometer in the time domain

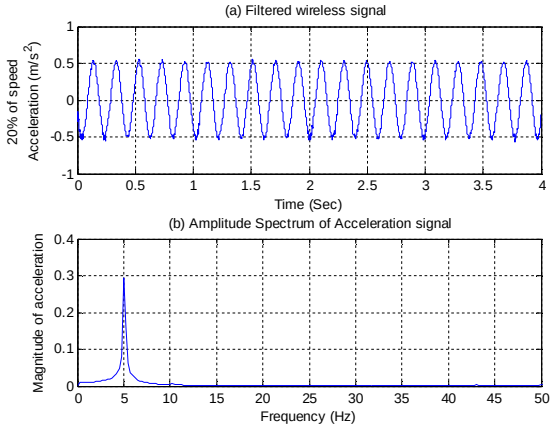

Figure 9 Filtered acceleration signal in the time and frequency domain

The IAS signal was calculated from the analogue signal of wireless accelerometer using FFT property given by the following equation (1):

$$\mathcal{F}\left\{\frac{d}{dt}\mathcal{X}(t)\right\} = \mathcal{J}\omega X(\omega) \qquad (1)$$

Since the acceleration *a(t)* can be obtained from the derivative of velocity. The relationship between acceleration and velocity can be rewritten as:

$$\mathcal{F}\{a(t)\} = \mathcal{J}\omega V(\omega) \qquad (2)$$

Consequently,

$$V(\omega) = \frac{1}{\mathcal{J}\omega}A(\omega) \qquad (3)$$

From equation (3) the variation in angular speed, i.e. IAS, can be obtained by computing the inverse FFT of the acceleration.

The IAS signal from wireless accelerometer was compared to the IAS measured by shaft encoder. The extraction of IAS signal from the encoder pulse used time-interval technique [5] according to the following steps:

1. Calculation of the time difference variation Δt of the encoder signal as shown in Figure 10.

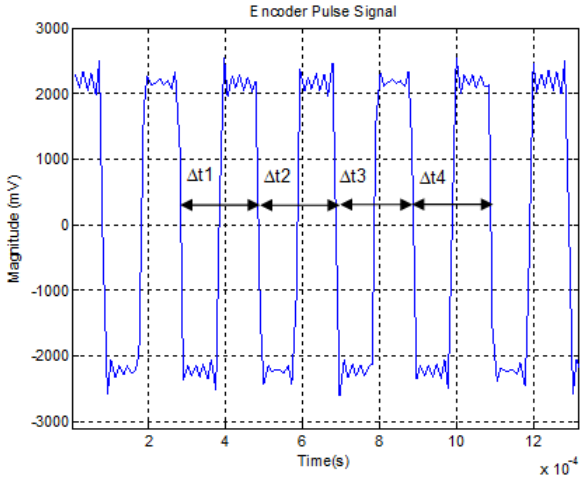

Figure 10 IAS raw data from encoder

2. The change in angular displacement Δθ can be computed knowing that the encoder generates 1000 pulses per revolution as:

$$\Delta\theta = \frac{2\pi}{1000} = 0.0063 \ (rad)$$

3. From step (1) and (2) the variation angular speed (IAS) can be derived using the equation below:

$$\omega = \frac{\Delta\theta}{\Delta t} \ (rad/sec) \qquad (4)$$

The variation of angular speed (ω) can be extracted from encoder signal using equation (4), as shown in Figure 11.

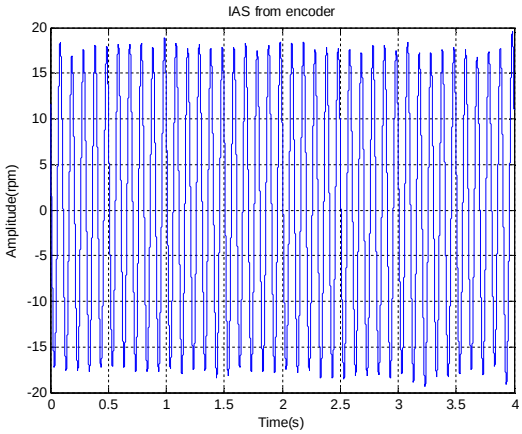

Figure 11 IAS waveform from encoder

Figure 12 presents the comparison of IAS signals extracted from both encoder and the wireless accelerometer when the test rig was run at 600 rpm. It can be observed that the profiles of the two waveforms are very similar. It confirms that wireless sensor can capture the dynamic behaviour of the rotor. However, the amplitude of the wireless sensor is lower. This may be caused by the difference in sensor positions and error in calibration process.

For making more detailed comparison, Figure 13 shows the normalised spectra for both encoder and wireless accelerometer IAS. From IAS shown in Figure 13(a), it can be seen that the rotational frequency and its higher order harmonics can be resolved by both signals. In addition, IAS from

wireless sensor shows lower noise level in high frequency range whereas it shows much higher amplitudes in low frequency range.

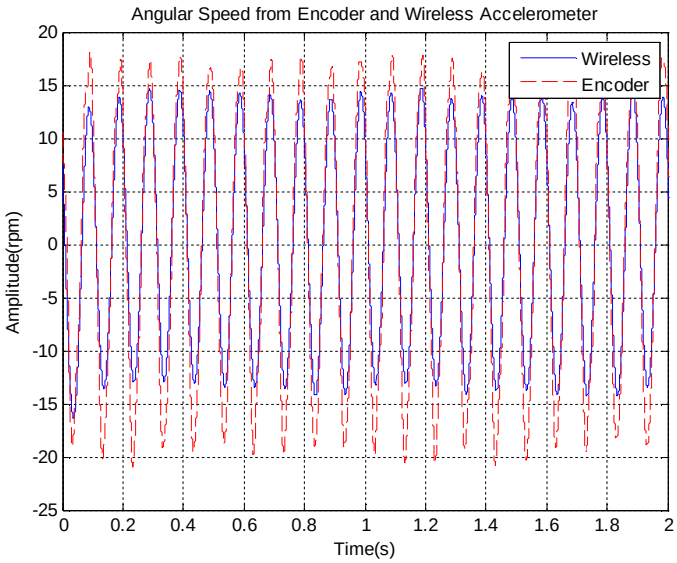

Figure 12 IAS waveform of wireless accelerometer and encoder

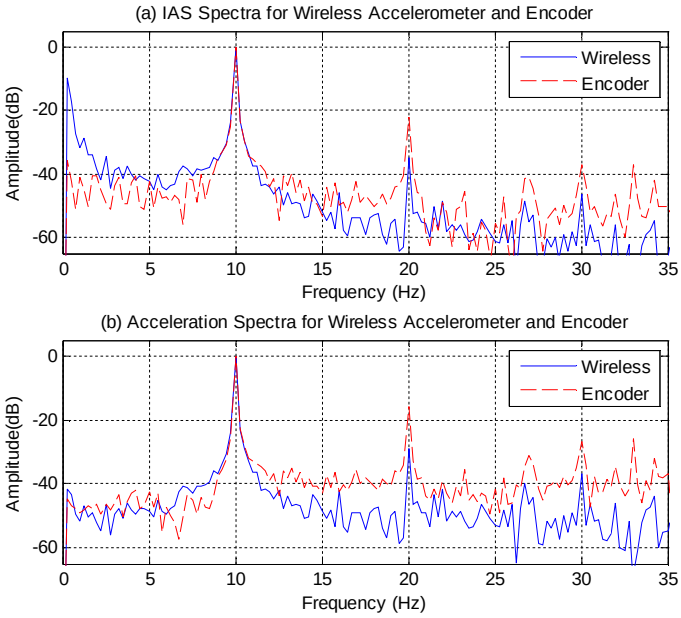

Figure 13 IAS Spectrum from wireless accelerometer and encoder

Further study shows that the high amplitude is due to numerical integration in calculating IAS. As shown by acceleration spectra in Figure 13(b), the amplitudes for both sensors are similar level in the low frequency range. Moreover, the high noise level is also observed in the graph. Therefore, it confirms that signal from wireless sensor has a higher signal-to-noise ratio, which allows detection of smaller fault.

5. **CONCLUSION**

The development of a wireless accelerometer is detailed and evaluated by measuring the IAS of a motor driving rotor. Although bandwidth of the developed wireless accelerometer is limited to 131.5

Hz by the active filter, the IAS from it shows consistent features with that from an encoder sensor. In addition, the wireless acceleration signal has less noise and it is more possible for small fault detection. Moreover, it has potential of measuring dynamic behaviour of the rotor. Future research will be conducted to expand the bandwidth and to evaluate the performance of fault diagnosis.

REFERENCES

[1] F. Andrés Bejarano, Jia Yi, Frederick Just. (2007), Crack Identification of a Rotating Shaft With Integrated Wireless Sensors. University of Puerto Rico, Mayaguez Campus, Mechanical Engineering Department, PO Box 9045, Mayaguez, Puerto Rico 00681-9045

[2] Analog Devices, Inc, ADXL202E Catalogue, at http://www.analog.com,2000.

[3] David M. Alter,Using PWM Output as a Digital-to-Analog Converter on a TMS320F280x Digital Signal Controller, DSP Applications – Semiconductor Group, Texas Instruments,SPRAA88A – September 2008

[4] Analysis of the Sallen-Key Architecture, July 1999 – Revised September 2002 Mixed Signal Products Application

[5] Ben Sasi, Y. A., (2005), The exploitation of Instantaneous Angular speed for Machinery condition monitoring, PhD Thesis, School of Mechanical, Aerospace and Civil Engineering, Manchester, UK.

[6] Sinocera Piezotronics, Inc. Copyright 2009 All Rights reserved http://www.china-yec.com/web(en)/product.htm

[7] Li, Y., Gu, F., Harris, D., and Ball, A. D., (2005) The Measurement of Instantaneous Angular Speed, International Journal of Mechanical Systems and Signal Processing,19(4) pp. 786-805.